ALMA MATER STUDIORUM
UNIVERSITÀ DI BOLOGNA

ARCHIVIO ISTITUZIONALE
DELLA RICERCA

Alma Mater Studiorum Università di Bologna
Archivio istituzionale della ricerca

Drug-in-cyclodextrin-in-polymeric nanoparticles: A promising strategy for rifampicin administration

This is the final peer-reviewed author’s accepted manuscript (postprint) of the following publication:

Published Version:
Drug-in-cyclodextrin-in-polymeric nanoparticles: A promising strategy for rifampicin administration / Angela Abruzzo, Vanessa Croatti, Giampaolo Zuccheri, Fiore Pasquale Nicoletta, Valentina Sallustio, Elisa Corazza, Beatrice Vitali, Teresa Cerchiara, Barbara Luppi, Federica Bigucci. - In: EUROPEAN JOURNAL OF PHARMACEUTICS AND BIOPHARMACEUTICS. - ISSN 0939-6411. - ELETTRONICO. - 180:(2022), pp. 190-200. [10.1016/j.ejpb.2022.10.001]

Availability:
This version is available at: https://hdl.handle.net/11585/899865 since: 2022-11-04

Published:
DOI: http://doi.org/10.1016/j.ejpb.2022.10.001

Terms of use:

Some rights reserved. The terms and conditions for the reuse of this version of the manuscript are specified in the publishing policy. For all terms of use and more information see the publisher's website.

This item was downloaded from IRIS Università di Bologna (https://cris.unibo.it/).
When citing, please refer to the published version.

(Article begins on next page)

19 April 2024

This is the final peer-reviewed accepted manuscript of:

Abruzzo A, Croatti V, Zuccheri G, Pasquale Nicoletta F, Sallustio V, Corazza E, Vitali B, Cerchiara T, Luppi B, Bigucci F. Drug-in-cyclodextrin-in-polymeric nanoparticles: A promising strategy for rifampicin administration. Eur J Pharm Biopharm. 2022 Nov;180:190-200. doi: 10.1016/j.ejpb.2022.10.001. Epub 2022 Oct 7. PMID: 36210035.

The final published version is available online at: **[https://doi.org/10.1016/j.ejpb.2022.10.001]**

Terms of use:

Some rights reserved. The terms and conditions for the reuse of this version of the manuscript are specified in the publishing policy. For all terms of use and more information see the publisher's website.

This item was downloaded from IRIS Università di Bologna (https://cris.unibo.it/)

When citing, please refer to the published version.

Authors' response to the Reviewer's comments

Manuscript Number: EJPB-D-22-00530

Drug-in-cyclodextrin-in-polymeric nanoparticles: a promising strategy for rifampicin administration

The authors would like to thank the reviewer for his/her comments which helped to improve the manuscript.

In the following all points of the reviewer are addressed, where first the reviewer's comment is repeated in italics and then replied to in plain text. Changes to the manuscript that have been made are marked with an underline.

1) Introduction. It is a common though to consider cyclodextrin cavity as hydrophobic, but is not actual the case. In fact, inside the cavity it is possible to host water molecules thus is better to say less hydrophilic. (for instance: Beilstein J Org Chem. 2019 Jul 17;15:1592-1600. doi: 10.3762/bjoc.15.163. eCollection 2019.)

We fully agree with the reviewer's comment and in the "Introduction" section, the sentence regarding the inner cavity of cyclodextrins and its ability to form inclusion complexes with drugs has been rewritten as "Cyclodextrins are cyclic oligosaccharides able to interact by means of their internal cavity with a large variety of drugs, mostly hydrophobic in nature, to form non-covalent inclusion complexes.".

2) Structures of the cross linking agents used should be reported and the NPs structure as well.

Structures of the crosslinking agents as well as of nanoparticles have been included in the graphical abstract.

3) Section 2.11. Please indicate the amount of the sample.

We thank the reviewer for reporting this oversight. In the "2.11 In vitro drug release" section, the amount of the sample taken from the medium has been introduced.

4) Section 3.2. The authors report that the formation of NPs are affected by several parameters. It this point connected to kinetic of the process or also to the final properties of the NPs?

In the text, we reported that the nanoparticle formation is influenced by CH and crosslinker concentration, the pH, and the time and speed of stirring. Regarding the employment of different CH/crosslinker weight ratios, we described that different amounts of crosslinker can lead to the

formation of clear solutions, opalescent suspensions, or aggregates (Table 1 of the manuscript), demonstrating that the amount of crosslinker is a crucial parameter to obtain suspensions characterized by a good grade of nanoparticle dispersion. As for the pH, and the time and speed of stirring, we did not correlate them with the final properties of the nanoparticles because they were chosen on the basis of our previous work, in which we have fine-tuned the ideal operating conditions to obtain crosslinked chitosan nanoparticles. In the revised manuscript we added the reference of the mentioned work.

5) The authors have analyzed the dimension of the NPs during the time. They have omitted to analyze the stability of the drug6) and also the release profile as well.

We thank the reviewer for the suggestion. We performed the antimicrobial activity test by using a remaining batch of nanoparticles which was stored for 180 days at +4-8 °C. Considering the low amount of this batch, the study was conducted only on *E. coli* for which a greater efficacy of nanoparticles had been measured at time zero.

As reported in the following table, after this storage period, nanoparticles were still effective with respect to rifampicin solution even if a reduction of activity was observed with respect to time zero.

Time (days)	RIF	CH/SBE-β-CD-RIF	CH/SBE-β-CD-RIF/CMC	CH/SBE-β-CD-RIF /TPP
0	4.50	1.08	0.58	0.72
180	4.50	2.15	1.16	1.43

However, we have decided to not include these additional data because we are planning a further study aimed to obtain freeze-dried nanoparticles starting from the suspension described in this work. We hypothesize that the freeze-drying process could improve the stability of nanoparticles preserving at the same time their functional properties (drug release ability, antimicrobial activity…).

6) Even much more important is the comparison of the release of the rifampicin by the new NPs and native SBE-CD to justify the necessity to prepare more complex NPs for the drug delivery

We thank the reviewer for the comment. However, the release of the drug from cyclodextrin does not meet the requirements described in the scope of the work. In fact, this research aims to develop a new drug delivery system able to join the benefits of the association of a drug-cyclodextrin complex with polymeric nanoparticles. Specifically, cyclodextrins have been chosen for their ability to act as a complexing agent, improving rifampicin solubility. On the other hand, chitosan nanoparticles have

been selected for their ability to modulate drug release, allowing less frequent dosing, and for their mucoadhesive ability able to enhance the residence time of the drug at the mucosal surface.

Highlights

Chitosan-based nanoparticles were prepared via the ionotropic gelation technique

A complex with sulphobutylether-β-cyclodextrin improved rifampicin solubility

The selection of a suitable crosslinker allowed to modulate nanoparticle properties

All developed nanoparticles showed mucoadhesive properties

Nanoparticles maintained drug antimicrobial activity against tested bacterial species

Graphical Abstract

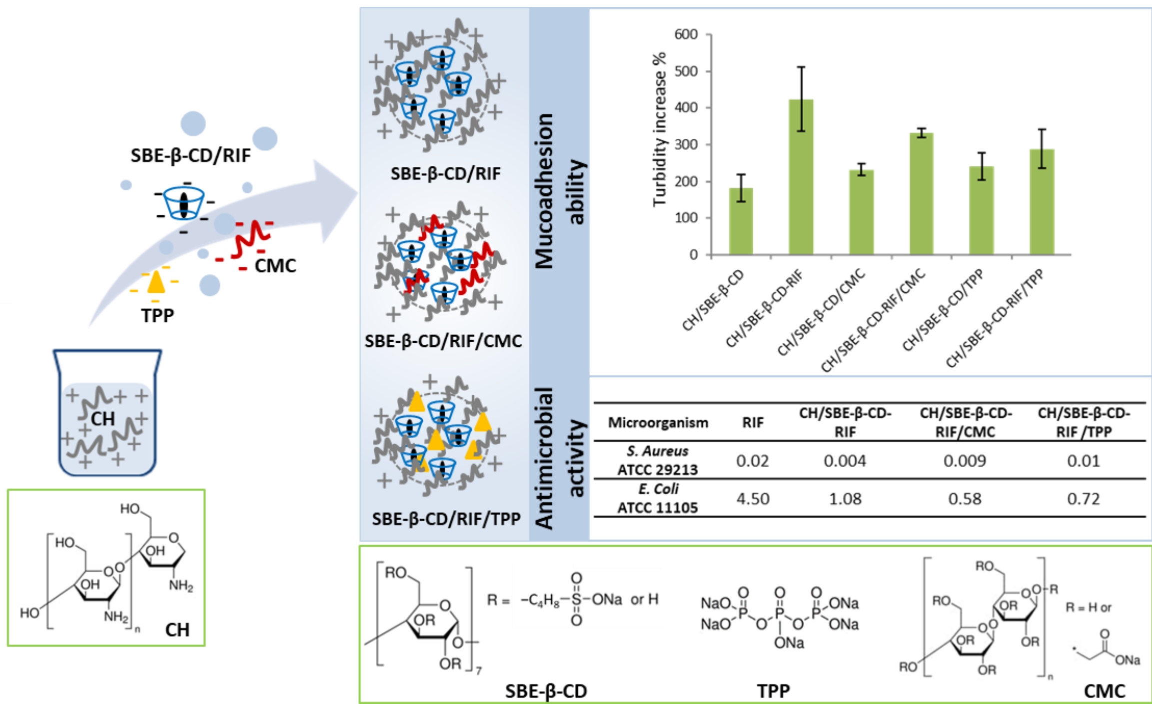

Microorganism	RIF	CH/SBE-β-CD-RIF	CH/SBE-β-CD-RIF/CMC	CH/SBE-β-CD-RIF /TPP
S. Aureus ATCC 29213	0.02	0.004	0.009	0.01
E. Coli ATCC 11105	4.50	1.08	0.58	0.72

Manuscript File
Click here to view linked References

Drug-in-cyclodextrin-in-polymeric nanoparticles: a promising strategy for rifampicin administration

Angela Abruzzo[a], Vanessa Croatti[a], Giampaolo Zuccheri[a,b,c], Fiore Pasquale Nicoletta[d], Valentina Sallustio[a], Elisa Corazza[a], Beatrice Vitali[a], Teresa Cerchiara[a], Barbara Luppi[a], Federica Bigucci[a*]

[a] Department of Pharmacy and Biotechnology, University of Bologna, Via San Donato 19/2, 40127 Bologna, Italy; E-mails: angela.abruzzo2@unibo.it; vanessa.croatti2@unibo.it; giampaolo.zuccheri@unibo.it; valentina.sallustio2@unibo.it; elisa.corazza7@unibo.it; b.vitali@unibo.it; teresa.cerchiara2@unibo.it; barbara.luppi@unibo.it; federica.bigucci@unibo.it.

[b] Interdepartmental Center for Industrial Research on Health Science and Technologies, Via Tolara di Sopra 41/E, 40064 Ozzano dell'Emilia, Bologna, Italy.

[c] S3 Center of the Nanoscience Institute of the Italian Research Council (CNRNANO), Via Campi, 213/A, 41125 Modena, Italy.

[d] Department of Pharmacy, Health and Nutritional Sciences, University of Calabria, Edificio Polifunzionale, 87036 Arcavacata di Rende, Cosenza, Italy; E-mail: fiore.nicoletta@unical.it.

*Author to whom correspondence should be addressed: Federica Bigucci, Department of Pharmacy and Biotechnology, Via San Donato 19/2, University of Bologna, 40127 Bologna, Italy. Tel: +39 051 2095615. E-mail: federica.bigucci@unibo.it

ABSTRACT

The aim of this work was to develop novel chitosan (CH) based nanoparticles (NPs) for rifampicin (RIF) delivery. RIF, a lipophilic molecule, was incorporated inside NPs as a complex with an anionic cyclodextrin, sulphobutyl-ether-β-cyclodextrin (SBE-β-CD). NPs were then prepared through the ionic gelation method by exploiting the interaction between CH and SBE-β-CD-RIF complex (CH/SBE-β-CD-RIF NPs), possibly in the presence of other crosslinkers, like carboxymethylcellulose (CH/SBE-β-CD-RIF/CMC NPs) and pentasodium tripolyphosphate (CH/SBE-β-CD-RIF/TPP NPs). NPs were then characterized for their size, ζ-potential, morphology, yield, drug loading, stability, mucoadhesion, *in vitro* drug release and antimicrobial activity. Results demonstrated that the functional properties of loaded NPs, like their size, ζ-potential, and stability, varied on the basis of the CH/crosslinker weight ratio. Interestingly, all the developed NPs had a round shape and were characterized by high yield values and mucoadhesive properties. Among them, NPs based on CH/SBE-β-CD-RIF and CH/SBE-β-CD-RIF/CMC have gained high drug loading, provided a sustained release of RIF and showed the best antimicrobial activity. Thus, both types of NPs may be considered as promising nanocarriers for the release of RIF.

Keywords:

Chitosan, nanoparticles, sulphobutyl-ether-β-cyclodextrin, rifampicin, mucoadhesion, antimicrobial activity

1. Introduction

Most of the available antimicrobial drugs display poor biopharmaceutical properties that limit their success in clinical applications. In particular, low solubility in aqueous media and high hydrolysis and enzymatic degradation compromise their effectiveness and the possibility of administration through traditional routes.

Rifampicin (RIF) is a semisynthetic antibiotic derivative of rifamycin that acts by inhibition of DNA-dependent RNA polymerase. It shows a very broad spectrum of activity against most Gram-positive (including *Staphylococcus aureus* and *Streptococcus pneumoniae*), some Gram-negative organisms (including *Escherichia coli* and *Pseudomonas aeruginosa*) and *Mycobacterium tuberculosis*, and is commonly administered for the treatment of infections caused by various microorganisms other than mycobacteria [1]. RIF presents moderate, variable bioavailability (under 70%) and it is classified as a class II drug of the Biopharmaceutic Classification System (BCS) for which rate and extent of dissolution are critical for an optimum bioavailability [2, 3].

In recent years, the use of cyclodextrins (CDs) in combination with nanotechnology has shown to be a promising strategy to improve drug bioavailability and develop optimized treatments for bacterial infections [4, 5]. Cycodextrins are cyclic oligosaccharides able to interact by means of their internal cavity with a large variety of drugs, mostly hydrophobic in nature, to form non-covalent inclusion complexes. These complexes can be used proficiently to improve the solubility, stability, dissolution rate and bioavailability of anti-infectives. In addition, CDs have gained importance because of their ability to promote drug internalization into cells and increase drug activity against bacteria [6].

Several studies showed that CDs can be successfully associated with other polymeric systems such as nanoparticles (NPs) to bypass the problems associated with both such carriers and join their relative benefits in a unique delivery system. Specifically, CDs have shown the ability to overcome the low capability of NPs to encapsulate lipophilic drugs, while NPs can improve the system stability and modulate the release of the loaded drug, thereby reducing the dose and frequency of administration [5].

Among polymeric systems, nano-sized systems based on chitosan (CH) are of great interest [7]. CH is a linear polysaccharide that consists of glucosamine and *N*-acetyl glucosamine units linked by β-1,4 linkages. It is the most widely applied biopolymer to prepare nanosystems not only for the presence of positive charges on its backbone at acidic pH, but also for its good biocompatibility and biodegradability, absence of toxicity, muco-adhesiveness and low cost. It holds GRAS status (Generally Recognised as Safe) from the United States Food and Drug Administration (US FDA) [8]. CH shows also an interesting antimicrobial activity mostly associated with the interaction with the negatively charged surface components of many microorganisms, causing extensive damages to the cell surface. Interestingly, the antimicrobial properties of CH can be increased by arranging the polymeric chains into NPs. This behaviour has been ascribed to the higher surface area-to-volume ratio leading to an increased density of positive charge on the NP surface and a better binding to the microbial cell walls and membranes [9, 10]. Finally, NPs can target antimicrobial agents to the site of infection, minimizing the amount of administrated drug and preventing the issues related to resistance [11].

CH NPs can be simply obtained in aqueous medium by ionotropic gelation using a negatively charged compound as crosslinking agent for positively charged CH [12]. As pointed out in our previous works, it is possible to use both low molecular weight multivalent anions and polymeric anions as cross-linking agents [13, 14].

This research aims to develop RIF loaded CH NPs through the ionotropic gelation technique, focusing on the use of different cross-linkers i.e., sulphobutylether-β-cyclodextrin (SBE-β-CD), sodium tripolyphosphate (TPP) and sodium carboxymethylcellulose (CMC). SBE-β-CD was chosen not only for the negative charges on sulfonate groups but also for the ability to act as a complexing and solubilizing agent for drugs. Moreover, it is cited in the FDA's list of Inactive Ingredients, and it is widely used in FDA-approved human products. [15]. TPP, a nontoxic salt with high charge density, is widely employed to cross-link polycationic polymers and represents one of the cross-linking agents of choice in preparing CH NPs [16]. CMC is a water-soluble and anionic polysaccharide commonly applied in food, cosmetic and pharmaceutical applications because of its cheapness, absence of toxicity and biodegradability [17].

To the best of our knowledge, up to now no studies have been published on the impact of association of an anionic CD to other cross-linking agents on the functional properties of CH NPs loading the anti-infective drug RIF. Briefly, the main steps of this study were: (a) to form an inclusion complex between SBE-β-CD and RIF; (b) to prepare CH NPs via ionotropic gelation technique using SBE-β-CD alone or in combination with TPP or CMC as polyanionic crosslinker; (b) to characterize the NPs in terms of size, polydispersity index, ζ-potential, morphology and drug encapsulation efficiency; (c) to investigate the NP mucoadhesion properties and drug release ability; (d) to confirm that RIF being incorporated in NPs maintains its antimicrobial activity against Gram-positive and Gram-negative bacterial species.

2. Materials and methods

2.1. Materials

Chitosan 85/5 (CH; MW 10-50 kDa, deacetylation degree 82.6% - 87.5%) was provided by Heppe Medical Chitosan GmbH (Saale, Germany). Sodium carboxymethylcellulose (CMC; MW 250 kDa, substitution degree 0.789) was obtained from A.C.E.F. (Piacenza, Italy). Sulphobutyl-ether-β-cyclodextrin sodium salt (SBE-β-CD, MW 2163 Da, substitution degree = 6.4) was a kind gift from CyDex, Inc. (San Diego, CA, USA). Rifampicin (RIF; MW 822.94 Da), pentasodium tripolyphosphate (TPP; MW 368 Da), mucin from porcine stomach (type II, bound sialic acid ~1%) and all other salts and solvents at analytical grade were purchased from Sigma-Aldrich (Milan, Italy). Phosphate buffer at pH 7.4 (PBS) was composed of 2.38 g/L $Na_2HPO_4 \times 12\ H_2O$, 0.19 g/L KH_2PO_4 and 8.00 g/L NaCl. Ultrapure water (18.2 MΩ cm) was obtained with a MilliQ apparatus by Millipore (Milford, MA, USA).

2.2. Rifampicin/Sulphobutyl-ether-β-cyclodextrin complex preparation

2.2.1. Phase solubility analysis

Phase solubility study was conducted following the method of Higuchi and Connors [18]. Specifically, an excess of RIF (10 mg) was added to 2 mL of ultrapure water containing SBE-β-CD at different concentrations (0-7.4 mM) in screw capped bottles. Each bottle was maintained under stirring (300 rpm) at +25 °C for 72 hours. Following equilibrium, the obtained dispersions were centrifuged (Microspin 12, Highspeed Mini-centrifuge, Biosan, Riga, Latvia) at 10,000 rpm for 15 minutes; the supernatants were isolated, filtered through a 0.22 μm pore size cellulose acetate filter (MF-Millipore Membrane, Tullagreen, Carrigtwohill, Co. Cork, Ireland) and assayed for the total dissolved RIF content by HPLC analysis after adequate dilution (see section 2.3). The phase solubility diagram was constructed by plotting concentrations of dissolved RIF against SBE-β-CD concentrations and the stability constant (k) was calculated as follows:

$$k = \frac{slope}{S_0 \times (1 - slope)} \qquad (1)$$

where S_0 represents the solubility of RIF in absence of CD.

2.2.2. Preparation and characterization of RIF/ SBE-β-CD soluble complex

For the incorporation of RIF inside the different polymeric nanoparticles (NPs), a soluble complex based on RIF and SBE-β-CD was prepared according to a previous procedure with slight modification [13]. Briefly, an excess amount of RIF (10 mg) was added to 2 mL of SBE-β-CD solution (3.7 mM) and the dispersion was left under magnetic stirring (300 rpm) at +25 °C for 72 hours. Subsequently, the dispersion was centrifuged and the supernatants were isolated, filtered (conditions described in section 2.2.1) and adequately diluted (see section 2.3). Finally, the samples were analyzed through HPLC to measure the dissolved amount of RIF.

To investigate the interaction between RIF and SBE-β-CD, a suitable amount of supernatant was freeze-dried (Christ Freeze-Dryer ALPHA1-2, Milan, Italy) and analyzed by differential scanning calorimetry (DSC). For these measurements, a Netzsch DSC200 PC differential scanning calorimeter (Netzsch, Germany) was used by setting the temperature from 30 °C to 350 °C and the heating rate of 10°C/min.

2.3 RIF quantification

RIF was quantified using HPLC-UV spectroscopy. The chromatographic system was composed of a Shimadzu (Milan, Italy) LC-10ATVP chromatographic pump and a Shimadzu SPD-10AVP UV-vis detector set at 254 nm. Separation was carried out on a Phenomenex (Torrance, CA, USA) Synergi Fusion-RP 80A (150 mm x 4.6 mm I.D., 5 mm) coupled to a Phenomenex Security Guard C18 guard cartridge (4 mm x 3.0 mm I.D., 5 mm). Manual injections of samples were performed using a Rheodyne 7125 injector with a 20 μL sample loop. The mobile phase was a mixture of KH_2PO_4 solution (10.2 mg/mL), citric acid solution (210.1 mg/mL), acetonitrile and methanol (26.6: 2.8: 51: 19.6, v/v). The flow rate was set at 0.4 mL/min. Data processing was

handled by means of a CromatoPlus computerized integration system (Shimadzu Italia, Milan, Italy). For the calibration curve construction, appropriate volumes of ethanolic solution of RIF were diluted with PBS (PBS/ethanol of 80:20 v/v), obtaining solutions with drug concentrations ranging from 0.25 to 40 μg/mL (good linearity was found; $R^2 = 0.9999$).

2.4 Preparation of unloaded and loaded NPs

NPs were prepared following a procedure previously reported [14], exploiting CH ability to interact with anionic molecules used as crosslinkers (ionotropic gelation technique). Briefly, a cationic phase was prepared by dissolving CH (0.67 mg/mL) in acetic acid (0.5 % v/v) for 24 hours under stirring at 200 rpm and adjusting the pH at 5.6 (pHmeter, MicroPH CRISON 2000, Carpi, Italy) with NaOH 2.5 % w/v. Crosslinking agents (SBE-β-CD, CMC and TPP) were separately solubilized in ultrapure water under stirring at 200 rpm for 30 minutes at different concentrations (8 mg/mL for SBE-β-CD and 2 mg/mL for CMC and TPP). To establish the conditions useful to obtain NPs (an opalescent dispersion without agglomeration or sedimentation), preliminary experiments were conducted. Specifically, anionic phases were prepared by mixing different volumes of SBE-β-CD solution with CMC or TPP solutions. Then, 0.5 mL of the final anionic phase was added to the cationic phase (1.5 mL) and maintained under stirring for 15 minutes. Finally, a visual examination of the obtained suspension was performed.

For the preparation of loaded NPs, the soluble complex, prepared as described in section 2.2.1, was used. Different volumes of the complex were mixed with CMC or TPP solutions and subsequently added to the cationic phase, thus obtaining NPs suspensions.

2.5 NP isolation and physicochemical characterization

NP suspensions, obtained as described in section 2.4, were centrifuged (Microspin 12, Highspeed Mini-centrifuge, Biosan, Riga, Latvia) on a glycerol bed at 14,000 rpm for 30 min at 25 °C. After supernatant discharging, the pellets composed of NPs were resuspended in ultrapure water and the size and ζ-potential of NPs were analyzed after appropriate dilution (1:20, v/v). Particle size and polydispersity index (PDI) were investigated at 25 °C by photon correlation spectroscopy (PCS) with a Brookhaven 90-PLUS instrument (Brookhaven Instruments Corp., Holtsville, NY, USA) and He-Ne laser beam at a wavelength of 532 nm (scattering angle of 90°). ζ-potential measurements were performed at 25 °C on a Malvern Zetasizer 3000 HS instrument (Malvern Panalytical Ltd., Malvern, UK).

2.6 Determination of yield

For yield determination, the NP suspensions were centrifuged without glycerol using the same conditions mentioned above (section 2.5); the supernatants were removed and the pellets were dried at 50 °C (heating

oven FD series, Binder, Tuttlingen, Germania) until constant weight. The yield of the process was calculated as follows:

$$yield\ (\%) = \frac{final\ solid\ weight}{theoretical\ solid\ weight} \times 100 \quad (2)$$

2.7 Determination of encapsulation efficiency and drug loading

For the calculation of the drug encapsulation efficiency (EE) and the drug loading (DL), loaded NPs were isolated as described in section 2.5 and the amount of non-entrapped RIF in the discharged supernatant was measured through HPLC. The EE (%) and DL (%) were calculated using the following equations:

$$EE\ (\%) = \frac{total\ amount\ of\ RIF - amount\ of\ non\ entrapped\ RIF}{total\ amount\ of\ RIF} \times 100 \quad (3)$$

$$DL\ (\%) = \frac{total\ amount\ of\ RIF - amount\ of\ non\ entrapped\ RIF}{NP\ weight} \times 100 \quad (4)$$

2.8 Morphology

The morphology of NPs was investigated with atomic force microscopy (AFM). AFM imaging was performed in air in PeakForce Tapping®-mode on a Multimode 8 Nanoscope system (Bruker) using ScanAsyst Air probes (Bruker, Karlsruhe, Germany). An aliquot of NP suspension of an appropriate concentration was layered on a disc of freshly cleaved mica and left to adsorb on the surface for about 10 min or longer. The sample was then mildly dried under a gentle flow of nitrogen gas. The adsorbed NPs were then imaged in air in different locations on the dried sample. Micrographs were only corrected by flattening their backgrounds (with the AFM manufacturer's software). The nanoparticle heights on the substrate were measured as an estimate of their diameter by employing a custom-written semi-automatic measurement software developed in Matlab (Mathworks, MA, U.S.A.). This automatically measures the distance of the highest point of user-selected nanoparticles from the substrate, thus avoiding the bias of defining selection thresholds and, at the same time, avoiding the variability due to the operator.

2.9 NP stability

NP stability was monitored by measuring the size and the PDI over 90 days of storage at +4-8 °C. At defined times (7, 15, 30, 60 and 90 days), aliquots of suspension were diluted in water (1:20 v/v) and NP size and PDI were determined using PCS.

2.10 Mucoadhesion properties

For the evaluation of NP mucoadhesive characteristics, turbidimetric measurements were carried out exploiting NP ability to interact with mucins [19, 14]. Firstly, mucin was dispersed in water (0.08 % w/v) for 24 hours and then the dispersion was centrifuged at 7500 rpm for 20 minutes to remove the undissolved protein. Samples obtained by mixing the mucin solution and NP suspension (1:3 v/v) were vortexed for 15 minutes and assayed for their turbidity at 650 nm (UV-Visible Spectrophotometer, Shimadzu Corporation, Australia). The absorbance (ABS) of mucin solution was used as control. The % increase in turbidity of the mixture mucin-NPs with respect to NPs suspensions was calculated as follows:

$$turbidity\ increase\ (\%) = \frac{ABS_{NPs+mucin} - ABS_{control}}{ABS_{NPs}} \times 100 \qquad (5)$$

2.11 In vitro drug release

To evaluate the release of RIF from the different NPs, 150 µL of NP suspensions were introduced in 2 mL of PBS at pH 7.4 and stirred at 200 rpm for 240 minutes. At predetermined time intervals (30, 60, 120, 240 minutes), aliquots of the sample (0.5 mL) were taken from the medium and centrifuged at 14,500 rpm for 15 minutes. The supernatants were filtered through a 0.22 µm pore size cellulose acetate filter and analyzed through HPLC after adequate dilution. RIF release over time was determined as M_t/M_0 (fractional amount), where M_t represents the amount of RIF released at each time and M_0 the total RIF mass loaded into the NPs.

2.12 Antimicrobial activity

NPs antimicrobial activity against *S. aureus* ATCC 29213 and *E. coli* ATCC 11105 was evaluated by using the broth microdilution method as reported in EUCAST guidelines [20]. Briefly, *S. aureus* and *E. coli* were aerobically cultured on Nutrient agar plates overnight at 37°C, afterwards, a bacterial suspension (10^6 CFU/mL) was prepared in Nutrient Broth (NB). RIF solution and RIF loaded in the three types of NPs (CH/SBE-β-CD-RIF, CH/SBE-β-CD-RIF/CMC and CH/SBE-β-CD-RIF/TPP) were tested in a 96-multiwell plate (Corning Inc., Pisa, Italy) considering a RIF concentration ranging from 55 µg/mL to 0.0002 µg/mL. Dilutions were prepared in sterile ultrapure water. Unloaded NPs were also tested considering the same range of dilutions. Wells were inoculated with 50 µL of bacterial suspensions along with 50 µl of samples and aerobically incubated at 37°C for 24 h. Bacterial growth control was prepared in sterile ultrapure water. A negative control (NB plus sterile ultrapure water) and sterility controls (NPs preparations plus NB) were included. Turbidity was read at EnSpire Multimode Plate Reader (PerkinElmer Inc., Waltham, MA) and minimal inhibitory concentration (MIC) was defined in relation to microorganism growth controls.

2.13 Statistical analysis

All the experiments were performed in triplicate. The results were expressed as mean ± standard deviation (S.D.). For all the performed studies, Student's t-test was used to determine statistical significance. Differences were deemed significant for $p < 0.05$.

3. Results and discussion

3.1 RIF/ SBE-β-CD complex preparation

In this study, SBE-β-CD was employed as solubilizing agent and crosslinker to include RIF, a poorly soluble drug, in polymeric NPs. In fact, it is well-known that the lipophilic inner cavity of CDs is able to form inclusion complexes with hydrophobic molecules, thus increasing their stability and solubility [21, 22]. Moreover, it was possible to take advantage of the ability of SBE-β-CD negative charges to interact with the positive charges of CH, in order to promote NP formation. At the same time, this interaction can favor the inclusion of lipophilic drugs inside hydrophilic systems like chitosan NPs. In our previous study, we demonstrated the ability of SBE-β-CD to include a low molecular-weight lipophilic compound, curcumin, and to allow its incorporation inside chitosan-based NPs [13]. In addition, in recent years, SBE-β-CD has been widely exploited for the preparation of CH based NPs for the delivery of different molecules (e.g. lactoferrin, cinnamaldehyde, ibrutinib, raloxifene) [23-26].

3.1.1. Phase solubility analysis

To evaluate the ability of SBE-β-CD to increase RIF solubility, phase solubility studies were performed. Fig. 1 shows the phase solubility diagram for the SBE-β-CD-RIF inclusion complex. As it can be seen, the solubility of RIF linearly increased with the increase of the concentration of SBE-β-CD (as demonstrated by the value of $R^2 = 0.9982$). Specifically, at +25 °C the solubility of RIF increased from 1.33±0.01 mM (1.09 ± 0.01 mg/mL) in absence of CD (S_0) [2, 27] to 2.99±0.12 mM (2.46 ± 0.10 mg/mL) in the presence of a CD concentration equal to 7.40 mM.

From the data in Fig. 1, it was also possible to evidence the formation of a soluble complex, with a stoichiometry of 1:1 (type A_L diagram). Finally, the measured stability constant was 216 M^{-1}, which is in the range (50-2000 M^{-1}) generally considered favorable for good interaction between the CD and the guest molecule [28].

3.1.2. Preparation and characterization of RIF/ SBE-β-CD soluble complex

The preparation of the soluble complex enabled to obtain a solution containing free RIF molecules, in equilibrium with those complexed within the CD cavity. The method consists of the preparation of SBE-β-CD aqueous solution to which an excess amount of RIF was added. After the equilibrium was reached, the excess of undissolved RIF was removed by centrifugation and filtration. The isolated solution (containing free RIF and SBE-β-CD-RIF soluble complex) was analyzed in terms of RIF concentration and used for the preparation

of loaded NPs. Specifically, the preparation of the soluble complex allowed to obtain a solution with a RIF concentration equal to 1.78±0.04 mg/mL (2.17±0.05 mM), which is higher than the RIF solubility (S_0, see section 3.1.1). In this context, the use of a solution containing a greater amount of RIF represents an advantageous approach to improve the loading of such a lipophilic drug inside a hydrophilic structure, like chitosan-based NPs.

To confirm the formation of the SBE-β-CD-RIF complex, the solid SBE-β-CD-RIF complex was obtained by freeze-drying and analyzed by DSC analysis. Fig. 2 shows the thermograms of RIF, SBE-β-CD, and SBE-β-CD-RIF complex. RIF directly decomposed at 255 °C, indicating the presence of the drug as polymorphic form I, in agreement with previous works [29]. In the case of SBE-β-CD, no well-defined melting point was detected demonstrating the amorphous nature of CD; moreover, a decomposition event was observed at 235 °C [30]. The disappearance of the decomposition event of RIF for SBE-β-CD-RIF complex evidenced the inclusion of the drug into the CD cavity [31].

3.2 Preparation of unloaded NPs

NPs were obtained by employing the ionotropic gelation method taking advantage of CH capacity to interact with anionic molecules. In detail, the method involved the preparation of a cationic phase based on CH solution and an anionic phase, which consisted of SBE-β-CD, possibly in association with other crosslinkers, such as TPP or CMC. In fact, the possibility to ionically crosslink CH with different anionic molecules, such as alginate, phytic acid, TPP or CMC was recently evaluated. This demonstrated the possibility to obtain NPs with specific size, surface charge and functional properties on the basis of their composition. Particularly, among all the formulations, NPs with the best functional properties were those based on CH/TPP and CH/CMC [14].

In spite of the relevant advantages of the method, which permitted to obtain NPs in an easy and simple way without the use of organic solvent, NP formation was influenced by several parameters, such as the CH and crosslinker concentration, the pH, the time and the speed of agitation [14, 32, 33]. In our study, the pH of the final suspension, which was around 5.6, guaranteed the ionization of CH amino groups (pKa 6.3), SBE-β-CD sulphate groups (more than six sulfate charges per mol according to the substitution degree) [34], CMC carboxylic groups (pKa= 4.3) [35] and TPP phosphate groups ($pKa_3 = 2.8$, $pKa_4 = 6.5$ and $pKa_5 = 9.2$) [36]. Moreover, we tested different CH/crosslinkers weight ratios (see Table 1) to select the most suitable ones for NP development and isolation. The use of different amounts of crosslinkers can lead to the formation of a clear solution, an opalescent suspension or an aggregate as a function of the interaction degree between CH and the anionic molecules. From the data reported in Table 1, it is possible to derive that the final suspension was clear in the presence of low amounts of crosslinkers, indicating the absence of NPs or very low yield. On the other hand, higher amounts of anionic molecules led to the formation of opalescent suspensions or aggregates. The appearance of opalescence was attributed to a satisfactory amount of NPs [33], while the formation of aggregates could be attributed to the presence of a high content of negative charges reducing the spatial

distance between polymer chains and consequently increasing the crosslinking density [13, 14, 34, 37, 38]. Moreover, when a combination of SBE-β-CD and CMC or TPP was used as anionic phase, a different behavior was observed. For a fixed amount of SBE-β-CD, it was possible to obtain an opalescent suspension or agglomerates with an equal content of CMC and TPP, respectively. This result suggested a higher crosslinking ability of low molecular weight crosslinkers, like TPP, with respect to CMC, in agreement with our previous data [14].

Taking these preliminary data into account, defined CH/crosslinkers weight ratios (marked with an asterisk in Table 1) were selected. The resulting opalescent suspensions were further investigated for the evaluation of the particle size, PDI, ζ-potential and yield. Moreover, the selected ratios were employed to obtain loaded NPs, by replacing SBE-β-CD with the complex.

3.3 NP physico-chemical characterization

The determination of particle size is a crucial step considering that it has been reported that the NP size influenced drug release and consequently the biological performance [39]. In Tables 2 and 3 the size of unloaded and loaded NPs is reported, respectively. Regarding unloaded NPs (Table 2), the size ranged from 201.6 ± 24.5 nm to 324.1 ± 13.3 nm. Among all the formulations, the highest size was measured in the case of CH/SBE-β-CD NPs, probably due to the presence of a greater amount of anionic crosslinker (CH/crosslinkers weight ratio 1:1.2) with respect to CH/SBE-β-CD/CMC NPs (CH/crosslinkers weight ratio 1:0.8) and CH/SBE-β-CD/TPP NPs (CH/crosslinkers weight ratio 1:0.5). However, despite the higher CH/crosslinkers weight ratio for CH/SBE-β-CD/TPP NPs with respect to CH/SBE-β-CD/CMC NPs, no significant difference was observed between these kinds of NPs ($p > 0.05$), probably due to a balancing phenomenon among the high crosslinking ability of TPP and the content of the anionic molecules.

The same behavior was also obtained for loaded NPs (Table 3). Moreover, for all the loaded formulations, a slight increase in size was observed with respect to the unloaded ones ($p < 0.05$), as consequence of the encapsulation of the complex inside the nanosystems [40]. In fact, the presence of the complex could contribute to the formation of a less compact structure due to an increased spatial distance between polymer chains and crosslinkers. Additionally, among all the loaded NPs, the presence of an increasing amount of drug (see DL results in section 3.5 and Table 3) led to the formation of NPs with a larger structure, so that CH/SBE-β-CD-RIF NPs, bearing the highest drug content, showed the largest size.

The measurement of PDI was performed in order to estimate the uniformity of the samples. Generally, it has been reported that, in the case of CH-based NPs, samples characterized by PDI values below 0.3 could be considered homogeneous [41]. As it can be seen from Tables 1 and 2, unloaded and loaded NPs displayed relatively narrow particle size distribution, as demonstrated by the relatively low PDI values.

Finally, the ζ-potential was determined considering that the surface charge of NPs can influence different NPs properties, such as stability, mucoadhesion characteristics and antibacterial activity. In fact, it is well known that high value of ζ-potential could determine a sufficient repulsion between the NPs, enough to avoid their

aggregation over the storage period [42]. Recently, it has been stated that NPs with ζ-potential in the range of 20-40 mV had an adequate repulsive force to remain disperse in aqueous environment [43]. Moreover, the presence of positive surface charges could strengthen the interaction between NPs and the mucus, by exploiting the ionic interaction between the positively charged groups and the negatively charged groups of sialic residues of mucin [44]. Finally, it has been reported that NPs with positive charges could bind efficiently to the negatively charged surface of bacteria, thus exercising antimicrobial activity especially against Gram-negative pathogens [45].

Data reported in Tables 2 and 3 indicated that all the developed NPs showed a positive ζ-potential, demonstrating that the positively charged groups of CH are mainly located on the NP surface [46]. Moreover, for loaded NPs, a higher positive ζ-potential was measured with respect to that of unloaded ones ($p < 0.05$, with except for CH/SBE-β-CD-RIF/TPP NPs), probably due to the presence of additional positive charges related to RIF. In fact, RIF is a zwitterionic molecule with a pKa_1 of 1.7 related to the 4-hydroxyl group and a pKa_2 of 7.9 related to the 3-piperazine nitrogen, and an isoelectric point at pH 4.8 in aqueous solution [2]. Furthermore, it has been reported that, when RIF was complexed with CD, the most energetically favorable conformation was with piperazine ring projected outward the CD cavity [31]. The presence of the positive charges on the piperazine nitrogen, located outside the cavity, could explain the increase of the net surface charge of loaded NPs with respect to the unloaded ones. Finally, in the case of loaded CH/SBE-β-CD-RIF/TPP NPs the increase of the ζ-potential value was not evident if compared with the respective unloaded NPs, probably as consequence of the presence of a low amount of drug (see DL data reported in section 3.5).

3.4 Determination of yield

The evaluation of the process yield represents a fundamental step since it has been generally recognized that high yields are favorable in order to contain the production costs. As displayed in Tables 2 and 3, no significant difference was observed between the different compositions as well as between unloaded and loaded NPs (medium values equal to 62.7% and 58.4% for unloaded and loaded NPs, respectively). Moreover, the obtained yield values were greater or in line with previous results concerning CH-CD based NPs [13, 34, 47-49]

3.5 Determination of encapsulation efficiency and drug loading

EE and DL values are shown in Table 3. As it can be seen, no significant differences were observed between the EE (%) values of the prepared NPs ($p > 0.05$) and the medium value was equal to 37.8 %. However, in consideration of the different volumes of soluble complex used for NPs preparation, a different concentration of RIF was obtained for all the samples. Particularly, the final RIF concentration inside loaded NPs was 55.6 ± 8.8 μg/mL, 26.0 ± 3.8 μg/mL and 14.6 ± 3.1 μg/mL for CH/SBE-β-CD-RIF NPs, CH/SBE-β-CD-RIF/CMC NPs and CH/SBE-β-CD-RIF/TPP NPs, respectively. Considering the DL (%) values, it can be assumed that among all the developed NPs, CH/SBE-β-CD-RIF NPs showed the highest DL (%) value ($p< 0.05$), while

CH/SBE-β-CD-RIF/TPP NPs showed the lowest one ($p < 0.05$). It can be concluded that the RIF concentration inside NPs increased with the increase of the amount of complex. This finding was in line with previous data reporting that the lower was the CD amount able to interact with CH and consequently to form NPs, the lower was the drug content [49]. Similarly, the work of Thanh Nguyen and Goycoolea demonstrated that as the amount of SBE-β-CD increased, the amount of complex with lipophilic flavonoids and their loading inside NPs increased [34].

3.6 Morphology

Atomic force microscopy (AFM) analysis was performed in order to gather information about the morphology of NPs, their size dispersion and to get some insight on their propensity to aggregate. The analysis of all specimens confirmed the presence of NPs and from the adsorption yield on the substrates used for sample preparation (freshly cleaved muscovite mica), it is confirmed that the average surface charge of NPs is positive. The AFM analysis that was performed relies on the electrostatic (or non-specific) adsorption of NPs on a flat substrate and it might turn out to display more efficiently those particles that have a better propensity for adsorption, when heterogeneous populations are assayed.

When analyzing CH/SBE-β-CD NPs, CMC/SBE-β-CD NPs or TPP/SBE-β-CD NPs, a large fraction of the imaged NPs was in the size range of 100-200 nm (estimated diameter). While CH/SBE-β-CD NPs also displayed significantly smaller particles, possibly free CH chains, (Fig. 3A), the most significant component was monodispersed and had an average diameter of about 200 nm. The main components of CH/SBE-β-CD/TPP NPs and CH/ SBE-β-CD/CMC NPs were monodispersed particles of apparent diameters between 100 and 150 nm. All particles showed a slight tendency towards aggregation (Fig. 3B and 3C). The individual NPs had a round shape.

It is possible that the measured height of the NPs on the substrate could represent an underestimation of the NPs size both due to some partial dehydration and some deformation inherent in the surface adsorption.

3.7 NP stability

The determination of NP stability represents a crucial aspect in consideration of a future development at industrial scale. Moreover, in the field of antibiotic delivery through nanosystems, the stability is very important, since it maximizes the number of NPs covering the surface of bacteria [34].

In order to analyze their stability, loaded NPs were stored for 90 days at +4-8°C and the size and the PDI were monitored. The size change during the storage period can be ascribed to many factors, such as particle aggregation, interaction of free polymer chains or crosslinkers with the NPs, and swelling related to the presence of hydrophilic or charged groups able to mediate the entry of water [50, 51]. As previously discussed, one of the critical parameters that influences the stability of NPs, in terms of their general tendency to

aggregate, is their ζ-potential. Generally, a large value of ζ-potential favors NP repulsion and consequently provides a good stability over time [42].

Fig. 4 shows the size change of loaded NPs over the tested time. As it can be seen, CH/SBE-β-CD-RIF NPs maintained their size during 90 days of storage, while in the case of CH/SBE-β-CD-RIF/TPP NPs a slight increase in size was observed ($p < 0.05$), reaching a final dimension equal to 326.2 ± 15.7 nm (from 245.1 ± 9.5 nm). Instead, CH/SBE-β-CD-RIF/CMC NPs displayed an evident increase in size after 30 days of storage with respect to time zero ($p < 0.05$), reaching after 90 days of storage a final size equal to 556.6 ± 34.0 (from 270.5 ± 16.3 nm). This result is closely linked to the surface charge of NPs. In fact, CH/SBE-β-CD-RIF NPs, endowed with the highest positive ζ-potential, were characterized by the best stability profile. This result agreed with previous works reporting the possible role of CD in particle stabilization [52, 53]. In the case of CH/SBE-β-CD-RIF/CMC NPs the significant increase in size could be related to the presence of CMC. In fact, in agreement with previous research studies [14, 54], the presence of polymeric crosslinkers, like CMC, composed of hydrophilic and negatively charged carboxylic groups, could increase the water uptake of the structure, and determine a greater hydrodynamic diameter. Finally, the PDI values were maintained lower than 0.3 (with the exception of CH/SBE-β-CD-RIF/CMC NPs after 60 days of storage), demonstrating a good homogeneity of the samples over the storage period (data not shown).

3.8 Mucoadhesion properties

Mucin, a protein with high molecular weight and heavy glycosylation, is generally secreted by different mucosal surfaces in many regions of the body, including the eyes, the respiratory tract, the gastrointestinal tract and the reproductive organs. RIF could be absorbed through mucosal membranes, since it has been classified as a molecule with high permeability properties [2]. In this context, the development of NPs with mucoadhesive properties could allow for an increased retention time of the drug at the specific site, thus improving its absorption and efficacy.

For this reason, the mucoadhesive ability of NPs was evaluated by measuring their ability to interact with mucin. NPs suspensions were mixed with mucin and the increase in turbidity occurred as consequence of the interaction between the mucin and the NPs was calculated (Fig. 5). As it can be seen, all the NPs determined an increase in turbidity, which demonstrated their ability to interact with mucin. This result can be generally explained by the positive surface charge of the NPs that promotes the interaction with the negative charges of the sulfonic acid and sialic acid residues of mucin [55-57]. Nevertheless, no significant difference ($p > 0.05$) was observed amongst the unloaded samples despite their different ζ-potential values (see Table 2). The same trend was also observed in the case of loaded NPs. This behavior could be attributed to different factors which at the same time influenced the NPs ability to interact with mucin. Particularly, the mucoadhesion ability could be ascribed to a balancing phenomenon between the surface charge and the size of NPs. For this reason, CH/SBE-β-CD NPs, despite their greatest ζ-potential value, possessed a similar mucoadhesive property to

other NPs, due to their greatest size which decreased the interaction with mucin. In fact, it is well-known that NPs of greater size can interact weakly with mucin, *in virtue* of their decreased surface area [55].

Finally, comparing unloaded and loaded NPs, a significantly higher mucoadhesion capacity was measured in the case of CH/SBE-β-CD-RIF NPs and CH/SBE-β-CD-RIF/CMC NPs with respect to the unloaded ones ($p < 0.05$). This can be attributed mainly to the higher ζ-potential of the loaded NPs than the unloaded ones. On the other hand, no significant difference was observed between the CH/SBE-β-CD-RIF/TPP NPs and CH/SBE-β-CD/TPP NPs ($p > 0.05$), possessing a similar ζ-potential.

Overall, our results demonstrated that all the developed NPs possessed mucoadhesive properties and are expected to have the ability to greatly increase the residence time of the drug at the mucosal surface, thus promoting its diffusion to the underlying epithelium and consequently its absorption [58].

3.9 In vitro drug release

Fig. 6 reports the *in vitro* release rate of RIF from the different NPs. As RIF was mainly complexed with CD, it can be assumed that the drug should dissociate from the complex to be released in the bulk medium. This was also reported by previous works, in which it has been described that the interaction between CD and the loaded drug has a crucial role in controlling the drug release [34, 25]. As it can be hypothesized, NPs provided a different behavior of drug release. Specifically, CH/SBE-β-CD-RIF/TPP NPs provided a fast release of RIF, reaching the 89% of the drug released after 60 minutes and a plateau after 120 minutes. Besides, a more sustained release of RIF was obtained from CH/SBE-β-CD-RIF NPs and CH/SBE-β-CD-RIF/CMC NPs, for which the plateau was reached after 180 minutes. This behavior can be probably attributed to a different interaction of CD (and consequently of the complex) with CH, in presence or not of other crosslinkers. In fact, it has been reported that TPP competed with SBE-β-CD in the interaction with CH [34]. In conclusion, in the presence of TPP, the SBE-β-CD-RIF complex could establish a weak interaction with CH leading to a rapid drug release. On the other hand, in the case of CH/SBE-β-CD-RIF/CMC NPs, the sustained release could be ascribed not only to the dissociation of the complex and the consequent repartition of free drug to the release medium, but also to drug diffusion through the polymeric network. In this case the presence of polymeric chains of CMC, through which RIF have to diffuse to reach the release medium, could further slow down the drug release.

The sustained release of RIF from CH/SBE-β-CD-RIF NPs and CH/SBE-β-CD-RIF/CMC NPs can be considered of fundamental importance, as it could allow less frequent dosing which, in turn, can help to obtain a better compliance and therapeutic efficacy [59].

3.10 Antimicrobial activity

MIC of free RIF and RIF loaded in the three types of NPs are reported in Table 4. Since RIF possesses an antimicrobial activity towards a broad spectrum of microorganisms, we used *S. aureus* ATCC 29213 and *E.*

coli ATCC 11105 as Gram-positive and Gram-negative model species, respectively. Free RIF demonstrated a good antibacterial activity towards *S. aureus* and *E. coli* showing MIC values of 0.02 µg/mL and 4.50 µg/mL, respectively. These results are in accordance to the MIC values of the antibiotic reported in literature for the two species tested [60, 61]. Interestingly, RIF loaded in all types of NPs had MIC values lower than its free form for both *S. aureus* and *E. coli*. In particular, towards *S. aureus*, NPs reduced MIC of RIF from 0.02 µg/mL to < 0.01 µg/mL (at least 2-fold reduction) with the best reduction exerted by CH/SBE-β-CD-RIF NPs (MIC: 0.004 µg/mL; 5-fold reduction). Regarding *E. coli*, NPs decreased the MIC value of free RIF at least 4-fold (from 4.5 µg/mL to < 1.08 µg/mL), reaching a reduction of almost 8-fold with CH/SBE-β-CD-RIF/CMC NPs (MIC: 0.58 µg/mL). No antimicrobial effect of unloaded NPs was registered for dilutions corresponding to the MIC values of RIF in NPs. These results demonstrated that all types of NPs enhanced the antimicrobial effect of free RIF on *S. aureus* and *E. coli* and, notably, it was possible to identify the best performing type of NPs on each tested species. These results can be explained considering that CH is a natural antimicrobial compound and studies reported that CH NPs interfere with Gram-positive cell wall and disrupt the Gram-negative outer membrane enhancing the uptake of antibiotics [62, 7].

4. Conclusion

In this study, NPs composed of CH in association with SBE-β-CD and CMC or TPP were successfully developed for RIF delivery. The encapsulation of the lipophilic molecule RIF inside CH NPs was achieved through the preparation of an inclusion complex between RIF and SBE-β-CD, which also improved drug solubility. The influence of CH/crosslinker weight ratio on NP formation was estimated and the optimized compositions were then used for the preparation of loaded NPs, which possessed a range of size between 245 and 351 nm, a good polydispersity index and a positive ζ-potential. All the developed NPs showed interesting mucoadhesive characteristics, which can favor the extension of drug retention at the mucosa. Finally, among all the NPs, CH/SBE-β-CD-RIF NPs and CH/SBE-β-CD-RIF/CMC NPs were characterized by high drug loading capacity, demonstrated to provide a sustained release of RIF and possessed an increased antimicrobial activity against *S. aureus* and *E. coli*, respectively. The current outcomes of our study highlighted the possibility to exploit the designed NPs for RIF delivery.

CRediT authorship contribution statement

Abruzzo: Conceptualization, Methodology, Validation, Formal analysis, Investigation, Writing - original draft, Writing - review & editing. V. Croatti: Methodology, Validation, Formal analysis, Investigation, Writing - original draft. G. Zuccheri: Methodology, Writing - review & editing. A. Miti: Methodology, Validation, Investigation, Writing - original draft. V. Sallustio: Methodology, Investigation. E. Corazza: Methodology, Investigation. B. Vitali: Methodology, Writing - review & editing. T. Cerchiara: Writing - review & editing.

B. Luppi: Writing - review & editing. F. Bigucci: Conceptualization, Methodology, Writing - original draft, Writing - review & editing.

Declaration of Competing Interest

The authors declare that they have no known competing financial interests or personal relationships that could have appeared to influence the work reported in this paper.

Acknowledgments

The authors would also like to thank Giulia Santucci, Andrea Dall'Ara and Francesco Zangoli for their valuable contribution.

References

[1] C.-Y. Lee, C.-H. Huang, P.-L. Lu, W.-C. Ko, Y.-H. Chen, P.-R. Hsueh, Role of rifampin for the treatment of bacterial infections other than mycobacteriosis, J. Infect. 75 (2017) 395-408.

[2] C. Becker, J.B. Dressman, H.E. Junginger, S. Kopp, K.K. Midha, V.P. Shah, S. Stavchansky, D.M. Barends, Biowaiver monographs for immediate release solid oral dosage forms: rifampicin, J. Pharm. Sci. 98(7) (2009) 2252-2267.

[3] F. Tewes, J. Brillault, W. Couet, J.-C. Olivier, Formulation of rifampicin–cyclodextrin complexes for lung nebulization, J. Control. Release. 129 (2008) 93-99.

[4] D.A. Real, K. Bolaños, J. Priotti, N. Yutronic, M.J. Kogan, R. Sierpe, O. Donoso-González, Cyclodextrin-modified nanomaterials for drug delivery: classification and advances in controlled release and bioavailability, Pharmaceutics. 13(12) (2021) 2131.

[5] P. Mura, Advantages of the combined use of cyclodextrins and nanocarriers in drug delivery: a review, Int. J. Pharm. 579 (2020) 119181.

[6] J.C. Imperiale, A.D. Sosnik, Cyclodextrin complexes for treatment improvement in infectious diseases, Nanomedicine (Lond.). 10(10) (2015) 1621-1641.

[7] S. Rashki, K. Asgarpour, H. Tarrahimofrad, M. Hashemipour, M.S. Ebrahimi, H. Fathizadeh, A. Khorshidi, H. Khan, Z. Marzhoseyni, M. Salavati-Niasari, H. Mirzaei, Chitosan-based nanoparticles against bacterial infections, Carbohydr. Polym. 251 (2021) 117108.

[8] T. Kean, M. Thanou, Biodegradation, biodistribution and toxicity of chitosan, Adv. Drug Deliv. Rev. 62(1) (2010) 3-11.

[9] Z. Ma, A. Garrido-Maestu, K.C. Jeong, Application, Mode of action, and in vivo activity of chitosan and its micro- and nanoparticles as antimicrobial agents: a review, Carbohydr. Polym. 176 (2017) 257-265.

[10] D.R. Perinelli, L. Fagioli, R. Campana, J.K.W. Lam, W. Baffone, G.F. Palmieri, L. Casettari, G. Bonacucina, Chitosan-based nanosystems and their exploited antimicrobial activity, Eur. J. Pharm. Sci. 117 (2018) 8-20.

[11] R.Y. Pelgrift, A.J. Friedman, Nanotechnology as a therapeutic tool to combat microbial resistance, Adv. Drug Deliv. Rev. 65 (2013) 1803-1815.

[12] K.G. Desai, Chitosan nanoparticles prepared by ionotropic gelation: an overview of recent advances, Crit. Rev. Ther. Drug Carrier Syst. 33(2) (2016) 107-158.

[13] A. Abruzzo, G. Zuccheri, F. Belluti, S. Provenzano, L. Verardi, F. Bigucci, T. Cerchiara, B. Luppi, N. Calonghi, Chitosan nanoparticles for lipophilic anticancer drug delivery: development, characterization and in vitro studies on HT29 cancer cells, Colloids Surf. B Biointerfaces. 145 (2016) 362-372.

[14] A. Abruzzo, B. Giordani, A. Miti, B. Vitali, G. Zuccheri, T. Cerchiara, B. Luppi, F. Bigucci, Mucoadhesive and mucopenetrating chitosan nanoparticles for glycopeptide antibiotic administration, Int. J. Pharm. 606 (2021) 120874.

[15] V.J. Stella, R.A. Rajewski, Sulfobutylether-β-cyclodextrin, Int. J. Pharm. 583 (2020) 119396.

[16] I. Dmour, M.O. Taha, Natural and semisynthetic polymers in pharmaceutical nanotechnology, in: A.M. Grumezescu (Eds.), Organic Materials as Smart Nanocarriers for Drug Delivery. Elsevier, Amsterdam, 2018, pp. 35-100.

[17] V. Kanikireddy, K. Varaprasad, T. Jayaramudu, C. Karthikeyan, R. Sadiku, Carboxymethyl cellulose-based materials for infection control and wound healing: a review, Int. J. Biol. Macromol. 164 (2020) 963-975.

[18] T. Higuchi, K.A. Connors, Phase-solubility techniques, Adv. Anal. Chem. Instrum. 4 (1965) 117-212.

[19] A. Abruzzo, B. Giordani, C. Parolin, B. Vitali, M. Protti, L. Mercolini, M. Cappelletti, S. Fedi, F. Bigucci, T. Cerchiara, B. Luppi, Novel mixed vesicles containing lactobacilli biosurfactant for vaginal delivery of an anti-Candida agent, Eur. J. Pharm. Sci. 112 (2018) 95-101.

[20] EUCAST-The European Committee on Antimicrobial Susceptibility Testing, EUCAST reading guide for broth microdilution. https://www.eucast.org/fileadmin/s, 2022 (accessed 1 March 2022).

[21] M.E. Brewster, T. Loftsson, Cyclodextrins as pharmaceutical solubilizers, Adv. Drug Deliv. Rev. 59 (2007) 645–666.

[22] T. Loftsson, D. Duchene, Cyclodextrins and their pharmaceutical applications, Int. J. Pharm. 329 (2007) 1-11.

[23] R. Varela-Fernández, X. García-Otero, V. Díaz-Tomé, U. Regueiro, M. López-López, M. González-Barcia, M.I. Lema, , F.J. Otero-Espinar, Design, optimization, and characterization of lactoferrin-loaded chitosan/TPP and chitosan/sulfobutylether-beta-cyclodextrin nanoparticles as a pharmacological alternative for keratoconus treatment, ACS Appl. Mater. Interfaces. 13(3) (2021) 3559-3575.

[24] W. Zhu, J. Wu, X. Guo, X. Sun, Q. Li, J. Wang, L. Chen, Development and physicochemical characterization of chitosan hydrochloride/sulfobutyl ether-beta-cyclodextrin nanoparticles for cinnamaldehyde entrapment, J. Food Biochem. 44(6) (2020) e13197.

[25] L. Zhao, B. Tang, P. Tang, Q. Sun, Z. Suo, M. Zhang, N. Gan, H. Yang, H. Li, Chitosan/sulfobutylether-beta-cyclodextrin nanoparticles for ibrutinib delivery: a potential nanoformulation of novel kinase inhibitor, J. Pharm. Sci. 109(2) (2020) 1136-1144.

[26] Z. Wang, Y. Li, Raloxifene/SBE-beta-CD inclusion complexes formulated into nanoparticles with chitosan to overcome the absorption barrier for bioavailability enhancement, Pharmaceutics. 10(3) (2018) 76.

[27] D. He, P. Deng, L. Yang, Q. Tan, J. Liu, M. Yang, J. Zhang, Molecular encapsulation of rifampicin as an inclusion complex of hydroxypropyl-β-cyclodextrin: design; characterization and in vitro dissolution, Colloids Surf. B Biointerfaces. 103 (2013) 580-585.

[28] T. Loftsson, D. Hreinsdóttir, M. Másson, Evaluation of cyclodextrin solubilization of drugs, Int. J. Pharm. 302 (2005) 18-28.

[29] S. Agrawal, Y. Ashokraj, P.V. Bharatam, O. Pillai, R. Pachagnula, Solid-state characterization of rifampicin samples and its biopharmaceutic relevance, Eur. J. Pharm. Sci. 22 (2004) 127-144.

[30] L. Szente, I. Puskás, T. Sohajda, E. Varga, P. Vass, Z.K. Nagy, A. Farkas, B. Várnai, S. Béni, E. Hazai, Sulfobutylether-beta-cyclodextrin-enabled antiviral remdesivir: characterization of electrospun- and lyophilized formulations, Carbohydr. Polym. 264 (2021) 118011.

[31] Q.K. Anjani, J. Domínguez-Robles, E. Utomo, M. Font, M.C. Martínez-Ohárriz, A.D. Permana, Á. Cárcamo-Martínez, E. Larrañeta, R.F. Donnelly, Inclusion complexes of rifampicin with native and derivatized cyclodextrins: in silico modeling, formulation, and characterization, Pharmaceuticals (Basel). 15(1) (2022) 20.

[32] A. Abruzzo, T. Cerchiara, F. Bigucci, G. Zuccheri, C. Cavallari, B. Saladini, B. Luppi, Cromolyn-crosslinked chitosan nanoparticles for the treatment of allergic rhinitis. Eur. J. Pharm. Sci. 131 (2019) 136-145.

[33] T. Cerchiara, A. Abruzzo, M. di Cagno, F. Bigucci, A. Bauer-Brandl, C. Parolin, B. Vitali, M.C. Gallucci, B. Luppi, Chitosan based micro- and nanoparticles for colon targeted delivery of vancomycin prepared by alternative processing methods, Eur. J. Pharm. Biopharm. 92 (2015) 112-119.

[34] H. Thanh Nguyen, F.M. Goycoolea, Chitosan/Cyclodextrin/TPP Nanoparticles Loaded with Quercetin as Novel Bacterial Quorum Sensing Inhibitors, Molecules. 22 (2017) 1975.

[35] F. Bigucci, A. Abruzzo, B. Vitali, B. Saladini, T. Cerchiara, M.T. Gallucci, B. Luppi, Vaginal inserts based on chitosan and carboxymethylcellulose complexes for local delivery of chlorhexidine: preparation, characterization and antimicrobial activity, Int. J. Pharm. 478 (2015) 456-463.

[36] Y. Cai, Y. Lapitsky, Analysis of chitosan/tripolyphosphate micro- and nanogel yields is key to understanding their protein uptake performance, J. Colloid. Interface Sci. 494 (2017) 242-254.

[37] M. Lazaridou, E. Christodoulou, M. Nerantzaki, M. Kostoglou, D.A. Lambropoulou, A. Katsarou, K. Pantopoulos, D.N. Bikiaris, Formulation and in-vitro characterization of chitosan-nanoparticles loaded with the iron chelator deferoxamine mesylate (DFO), Pharmaceutics. 12 (2020) 238-254.

[38] R.A. Hashad, R.A. Ishak, S. Fahmy, S. Mansour, A.S. Geneidi, Chitosan-tripolyphosphate nanoparticles: optimization of formulation parameters for improving process yield at a novel pH using artificial neural networks, Int. J. Biol. Macromol. 86 (2016) 50-58.

[39] Y. Pan, J.M. Zheng, H.Y. Zhao, Y.J. Li, H. Xu, G. Wei, Relationship between drug effects and particle sizeof insulin-loaded bioadhesive microspheres, Acta Pharmacol. Sin. 23 (2002) 1051-1056.

[40] T. Cerchiara, A. Abruzzo, R.A. Ñahui Palomino, B. Vitali, R. De Rose, G. Chidichimo, L. Ceseracciu, A. Athanassiou, B. Saladini, F. Dalena, F. Bigucci, B. Luppi, Spanish Broom (Spartium junceum L.) fibers impregnated with vancomycin-loaded chitosan nanoparticles as new antibacterial wound dressing: preparation, characterization and antibacterial activity, Eur. J. Pharm. Sci. 99 (2017) 105-112.

[41] Y. Ciro, J. Rojas, M.J. Alhajj, G.A. Carabali, C.H. Salamanca, Production and characterization of chitosan-polyanion nanoparticles by polyelectrolyte complexation assisted by high-intensity sonication for the modified release of methotrexate, Pharmaceuticals (Basel). 13 (2020) 11.

[42] R.H. Müller, C. Jacobs, O. Kayser, Nanosuspensions as particulate drug formulations in therapy, Adv. Drug Deliv. Rev. 47 (2001) 3-19.

[43] S. Zhao, X. Yang, V.M. Garamus, U.A. Handge, L. Bérengère, L. Zhao, G. Salamon, R. Willumeit, A. Zou, S. Fan, Mixture of nonionic/ionic surfactants for the formulation of nanostructured lipid carriers: effects on physical properties, Langmuir. 30 (2014) 6920-6928.

[44] K. Netsomboon, A. Bernkop-Schnürch, Mucoadhesive vs. mucopenetrating particulate drug delivery, Eur. J. Pharm. Biopharm. 98 (2016) 76-89.

[45] Y.C. Chung, Y.P. Su, C.C. Chen, G. Jia, H.L. Wang, J.C. Wu, J.G. Lin, Relationship between antibacterial activity of chitosan and surface characteristics of cell wall, Acta Pharmacol. Sin. 25 (2004) 932-936.

[46] S.K. Khalil, G.S. El-Feky, S.T. El-Banna, W.A. Khalil, Preparation and evaluation of warfarin-β-cyclodextrin loaded chitosan nanoparticles for transdermal delivery, Carbohydr. Polym. 90 (2012) 1244-1253.

[47] Z. Alvi, M. Akhtar, N.U. Rahman, K.M. Hosny, A.M. Sindi, B.A. Khan, I. Nazir, H. Sadaquat, Utilization of gelling polymer to formulate nanoparticles loaded with epalrestat-cyclodextrin inclusion complex: formulation, characterization, in-silico modelling and in-vivo toxicity evaluation, Polymers (Basel). 13 (2021) 4350.

[48] F. Maestrelli, M. Garcia-Fuentes, P. Mura, M.J. Alonso, A new drug nanocarrierconsisting of chitosan and hydoxypropylcyclodextrin, Eur. J. Pharm. Biopharm. 63 (2006) 79-86.

[49] A.A. Mahmoud, G.S. El-Feky, R. Kamel, G.E.A. Awad, Chitosan/sulfobutylether--cyclodextrin nanoparticles as a potential approach for ocular drug delivery, Int. J. Pharm. 413 (2011) 229-236.

[50] T. López-León, E.L.S. Carvalho, B. Seijo, J.L. Ortega-Vinuesa, D. Bastos-González, Physicochemical characterization of chitosan nanoparticles: electrokinetic and stability behavior, J. Colloid Interface Sci. 283, (2005) 344-351.

[51] E.S.K. Tang, M. Huang, L.Y. Lim, Ultrasonication of chitosan and chitosan nanoparticles, Int. J. Pharm. 265 (2003) 103-114.

[52] A. Krauland, M. Alonso, Chitosan/cyclodextrin nanoparticles as macromolecular drug delivery system, Int. J. Pharm. 340 (2007) 134-142.

[53] A. Trapani, M. Garcia-Fuentes, M.J. Alonso, Novel drug nanocarriers combining hydrophilic cyclodextrins and chitosan, Nanotechnology. 19 (2008) 185101.

[54] H. Choukaife, A.A. Doolaanea, M. Alfatama, Alginate nanoformulation: influence of process and selected variables, Pharmaceuticals (Basel). 13 (2020) 335-368.

[55] E.M.A. Hejjaji, A.M. Smith, G.A. Morris, Evaluation of the mucoadhesive properties of chitosan nanoparticles prepared using different chitosan to tripolyphosphate (CS:TPP) ratios, Int. J. Biol. Macromol. 120 (2018) 1610-1617.

[56] A. Abruzzo, F.P. Nicoletta, F. Dalena, T. Cerchiara, B. Luppi, F. Bigucci, Bilayered buccal films as child-appropriate dosage form for systemic administration of propranolol, Int. J. Pharm. 531 (2017) 257-265.

[57] T. Cerchiara, A. Abruzzo, C. Parolin, B. Vitali, F. Bigucci, M.C. Gallucci, F.P. Nicoletta, B. Luppi, Microparticles based on chitosan/carboxymethylcellulose polyelectrolyte complexes for colon delivery of vancomycin, Carbohydr. Polym. 143 (2016) 124-130.

[58] D. Pawar, S. Mangal, R. Goswami, K.S. Jaganathan, Development and characterization of surface modified PLGA nanoparticles for nasal vaccine delivery: effect of mucoadhesive coating on antigen uptake and immune adjuvant activity, Eur. J. Pharm. Biopharm. 85(3) (2013) 550-559.

[59] D.L. Clemens, B.Y. Lee, M. Xue, C.R. Thomas, H. Meng, D. Ferris, M.A. Horwitz, Targeted intracellular delivery of antituberculosis drugs to Mycobacterium tuberculosis-infected macrophages via functionalized mesoporous silica nanoparticles, Antimicrob. Agents Chemother. 56 (5) (2012) 2535-2545.

[60] K.C. Reiter, G.E. Sambrano, B. Villa, T.G. Paim, C.F. de Oliveira, P.A. d'Azevedo, Rifampicin fails to eradicate mature biofilm formed by methicillin-resistant Staphylococcus aureus, Rev. Soc. Bras. Med. Trop. 45(4) (2012) 471-474.

[61] I. Stock, B. Wiedemannm, Natural antibiotic susceptibility of Escherichia coli, Shigella, E. vulneris, and E. hermannii strains, Diagn. Microbiol. Infect. Dis. 33(3) (1999) 187-199.

[62] I.R. Scolari, P.L. Páez, M.M. Musri, J.P. Petiti, A. Torres, G.E. Granero, Rifampicin loaded in alginate/chitosan nanoparticles as a promising pulmonary carrier against Staphylococcus aureus, Drug. Deliv. Transl. Res. 10(5) (2020) 1403-1417.

Fig. 1. Phase solubility diagram of SBE-β-CD-RIF complex.

Fig. 2. DSC thermograms of RIF, SBE-β-CD and SBE-β-CD-RIF complex.

Fig. 3. AFM micrographs of CH/SBE-β-CD-RIF NPs (A), CH/SBE-β-CD-RIF/CMC NPs (B) and CH/SBE-β-CD-RIF/TPP NPs (C).

Fig. 4. Variation of size of loaded NPs during 90 days of storage at +4-8 °C.

Fig. 5. Mucoadhesive properties of unloaded and loaded NPs.

Fig. 6. *In vitro* release of RIF from NPs.

Figure 1 Click here to access/download;Figure;Figure 1.docx

Figure 1

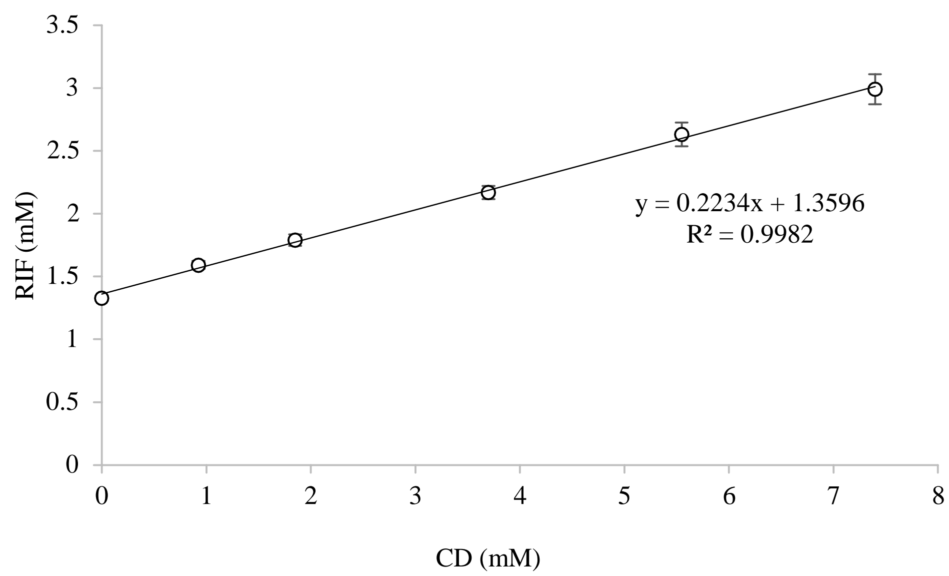

Figure 2

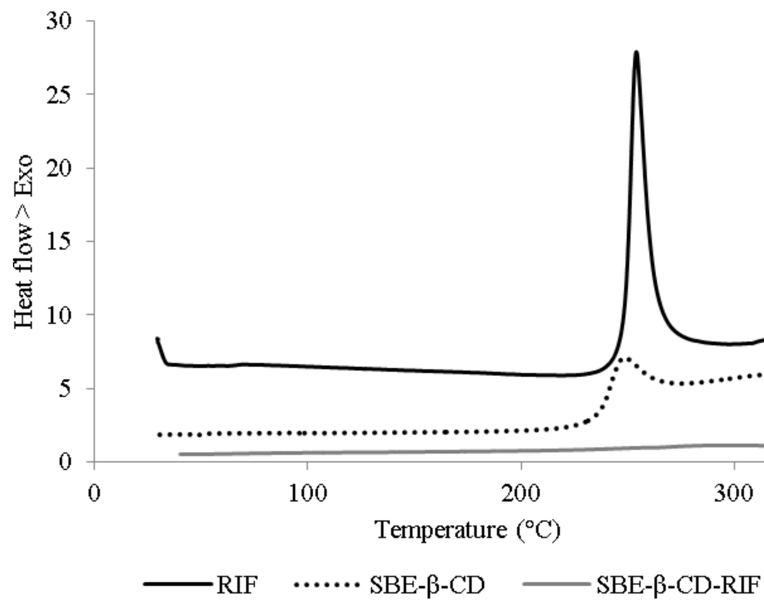

Click here to access/download;Figure;Figure 3.docx

Figure 3

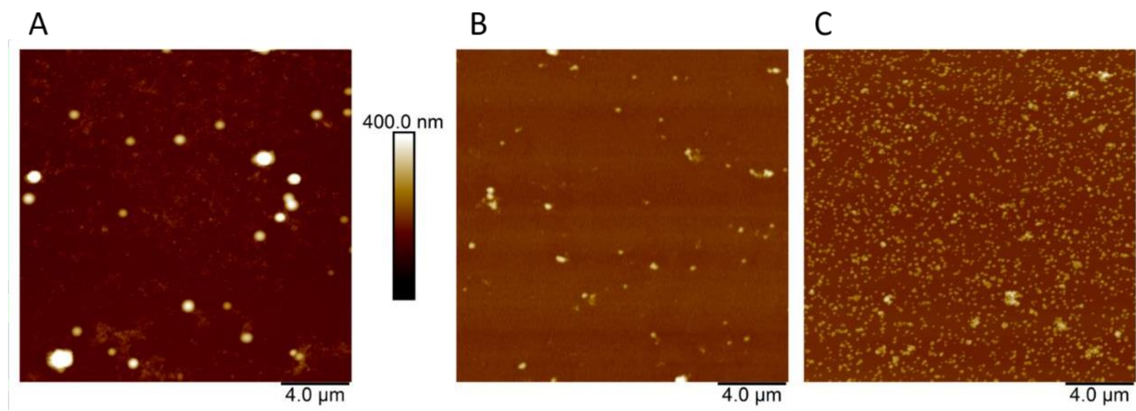

Figure 4

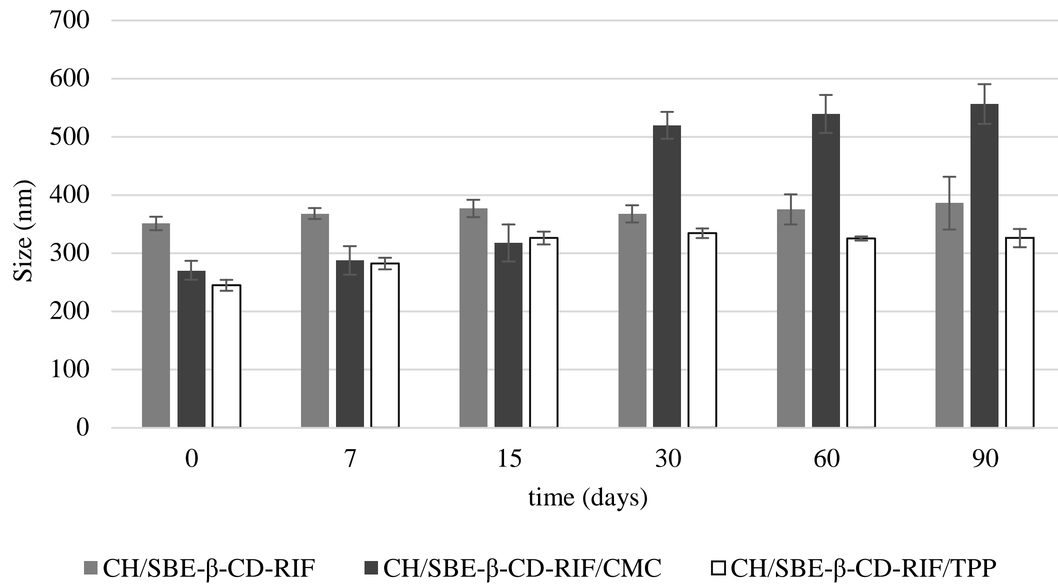

Figure 5

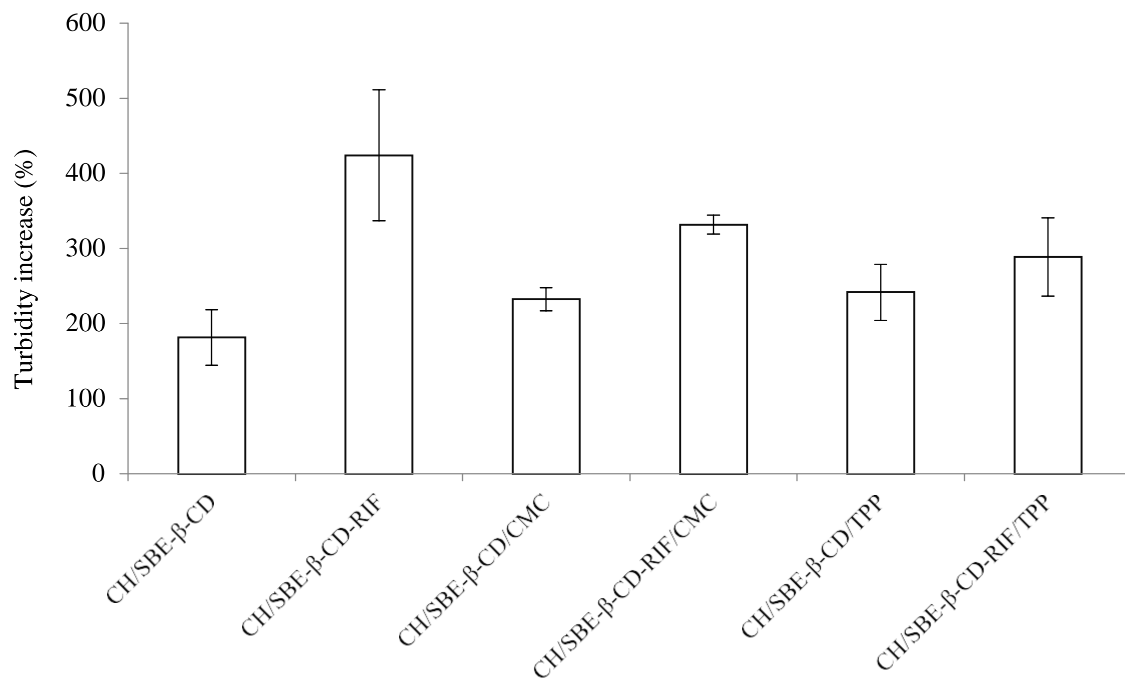

Click here to access/download;Figure;Figure 6.docx

Figure 6

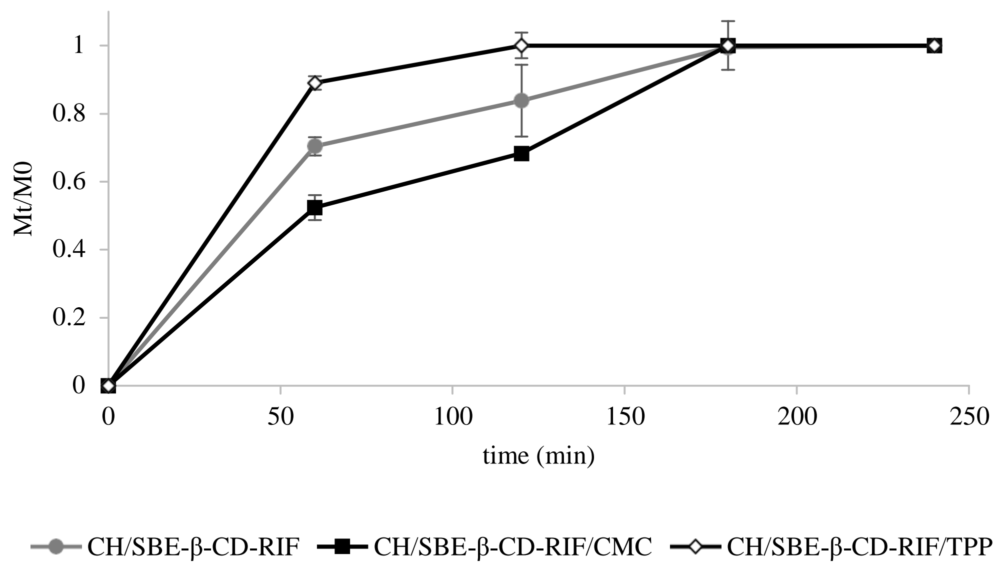

Table 1 Click here to access/download;Table;Tabella 1.docx

Table 1. Appearance of the final suspensions (1 ml) prepared with fixed amount of CH (0.5 mg) and different amounts (mg) of crosslinkers.

SBE-β-CD (mg)	CMC (mg)	TPP (mg)	CH/Crosslinker weight ratio	Appearance
1.6	-	-	1:3.2	Precipitation
1.2	-	-	1:2.4	Precipitation
1.0	-	-	1:2	Precipitation
0.8	-	-	1:1.6	Precipitation
0.6	-	-	1:1.2	Opalescent (*)
0.4	-	-	1:0.8	Slightly opalescent
0.2	-	-	1:0.4	Clear solution
0.4	0.1	-	1:1	Precipitation
0.3	0.2	-	1:1	Precipitation
0.3	0.15	-	1:0.9	Precipitation
0.3	0.1	-	1:0.8	Opalescent (*)
0.3	0.05	-	1:0.7	Slightly opalescent
0.2	0.1	-	1:0.6	Slightly opalescent
0.2	0.05	-	1:0.5	Clear solution
0.4	-	0.1	1:1	Precipitation
0.3	-	0.1	1:0.8	Precipitation
0.2	-	0.1	1:0.6	Precipitation
0.2	-	0.05	1:0.5	Opalescent (*)
0.2	-	0.02	1:0.44	Clear solution

(*) Selected CH/Crosslinker weight ratios for further studies and for the preparation of loaded NPs.

Table 2. Size (nm), polydispersity index (PDI), ζ-potential (mV) and yield (%) of the unloaded NPs.

Type of NPs	Size (nm)	PDI	ζ-pot (mV)	Yield (%)
CH/SBE-β-CD	324.1 ± 13.3	0.12 ± 0.01	+33.4 ± 2.8	66.1 ± 0.5
CH/SBE-β-CD/CMC	224.2 ± 14.9	0.07 ± 0.01	+23.8 ± 0.5	62.8 ± 4.2
CH/SBE-β-CD/TPP	201.6 ± 24.5	0.28 ± 0.01	+25.6 ± 0.8	59.3 ± 9.2

Table 3 Click here to access/download;Table;Tabella 3.docx

Table 3. Size (nm), polydispersity index (PDI), ζ-potential (mV), yield (%), encapsulation efficiency (EE %) and drug loading (DL %) of the loaded NPs.

Type of NPs	Size (nm)	PDI	ζ-pot (mV)	Yield (%)	EE (%)	DL (%)
CH/SBE-β-CD-RIF	351.2 ± 11.4	0.18 ± 0.04	+40.6 ± 1.5	62.2 ± 6.1	41.6 ± 6.6	7.7 ± 1.2
CH/SBE-β-CD-RIF/CMC	270.5 ± 16.3	0.12 ± 0.01	+29.5 ± 0.2	58.2 ± 0.5	38.9 ± 5.7	4.8 ± 0.7
CH/SBE-β-CD-RIF/TPP	245.1 ± 9.5	0.22 ± 0.08	+25.2 ± 1.4	54.9 ± 4.2	32.8 ± 7.0	3.5 ± 0.7

 Click here to access/download;Table;Tabella 4.docx

Table 4. MIC (μg/mL) of free RIF and RIF loaded in NPs.

Microorganism	RIF	CH/SBE-β-CD-RIF	CH/SBE-β-CD-RIF/CMC	CH/SBE-β-CD-RIF /TPP
S. aureus ATCC 29213	0.02	0.004	0.009	0.01
E. coli ATCC 11105	4.50	1.08	0.58	0.72